Available online at www.sciencedirect.com
SCIENCE DIRECT
Journal of Molecular Catalysis A: Chemical 243 (2006) 24–30
JOURNAL OF MOLECULAR CATALYSIS A: CHEMICAL
www.elsevier.com/locate/molcata

Influence of impregnation times on the dispersion of CuO on anatase

Haiyang Zhu [a], Yong Wu [a,c], Xi Zhao [a], Haiqin Wan [a], Lijuan Yang [a], Jianming Hong [b], Qing Yu [a], Lin Dong [a,*], Yi Chen [a], Can Jian [d], Jun Wei [d], Penghui Xu [d]

[a] *Key Laboratory of Mesoscopic Chemistry of MOE, College of Chemistry and Chemical Engineering, China*
[b] *Center of Modern Analysis, Nanjing University, Nanjing 210093, China*
[c] *Department of Chemistry, Nanjing Normal University, Nanjing 210097, China*
[d] *Department of Chemistry and Environment, Tibet University, Lhasa 850000, China*

Received 25 May 2005; received in revised form 12 August 2005; accepted 12 August 2005
Available online 5 October 2005

Abstract

X-ray diffraction (XRD), temperature-programmed reduction (TPR) and X-ray photoelectron spectroscopy (XPS) were employed to investigate the dispersion of copper oxide in CuO/TiO_2 samples prepared by one and double-step impregnations and the NO + CO activities of CuO/TiO_2 samples were also tested. The results indicate that the dispersion capacity of copper oxide in CuO/TiO_2 samples with one-step impregnation and double impregnations are about 0.52 and 0.98 mmol/100 m^2 TiO_2, respectively, which should be related to the shielding effect of accompanying NO_3^- anions during the impregnations. Therefore, the dispersion capacity of copper oxide on anatase with double impregnations could approach to 1.16 mmol/100 m^2 TiO_2, i.e. a value corresponding to the density of vacant sites on the (0 0 1) surface of TiO_2. The NO + CO activities of CuO/TiO_2 samples suggest that dispersed copper oxide species in these catalysts is the mainly active species and the increasing amount of dispersed copper oxide would enhance their activities. It seems to suggest that, for the supported catalysts, double or multiple impregnations would result in better activity than those prepared by one-step impregnation. In addition, the coordination environment of the dispersed copper oxide species existed on the anatase surface has been discussed by the incorporation model [Y. Chen, L.F. Zhang, Catal. Lett. 12 (1992) 51].

Keywords: Copper oxide species; Anatase; Dispersion capacity; Impregnation; Incorporation model

1. Introduction

The interactions between metal oxide and oxide support have drawn much attention due to the wide applications of supported metal oxide catalysts, such as hydrodesulfurization, cracking, polymerization, partial oxidation of hydrocarbons and the selective reduction of nitrogen oxides. Accordingly, a large number of studies have been devoted to exploring the interaction between the support and the dispersed oxide species, and various explanations or models concerning the nature of the interaction have been proposed [1–7].

TiO_2 is a very important support widely used in heterogeneous catalysis. Transition metal oxides supported on TiO_2 have found application in various industrial reactions, such as V_2O_5/TiO_2 in selective oxidation of *o*-xylene to phthalic anhydride [8], and the partial oxidation of hydrocarbons [9], $CoO–MoO_3/TiO_2$ for the hydrodesulfurization of hydrocarbon oils [10] and MoO_3/TiO_2 for the selective photooxidation of alcohol [11]. It is crucial for elucidating the nature of the catalysts and exploring the key factors in controlling the properties of the catalysts to investigate the interaction between the transition metal oxide and TiO_2 support.

The catalysts containing transition metals, especially copper, show a potential application for the treatment of exhaust gas from automobiles [12–15], complete oxidation of volatile organic compounds [16–19] and special attention has also been paid to this system as a substitute for noble metal containing catalysts recently [20]. Generally, three forms of the copper containing catalysts have been used for these investigations, e.g. unsupported copper oxide catalysts [21], supported copper oxide catalysts and supported metal copper catalysts [22,23]. As reported by Andersson and co-workers, the dispersed copper oxide on TiO_2 was active for the complete oxidation of CO and toluene. However, the presence of copper oxide species

* Corresponding author. Tel.: +86 25 83594945; fax: +86 25 83317761.
E-mail address: donglin@nju.edu.cn (L. Dong).

1381-1169/$ – see front matter © 2005 Elsevier B.V. All rights reserved.
doi:10.1016/j.molcata.2005.08.021

accelerates the sintering of TiO_2 support, which prohibits the application of these catalysts [18]. Xie et al. have investigated the dispersion of copper oxide on anatase and the influence of dispersed copper oxide on the phase transformation from anatase to rutile. Their results suggest that the dispersion capacity of copper oxide on anatase is about 4.0 Cu^{2+}/nm^2 TiO_2, i.e. 0.66 mmol/100 m^2 TiO_2 [24]. Unfortunately, there was not a further explanation and discussion for their value of the dispersion capacity rather than other values. In the actual uses of the supported catalysts preparation, the dispersion capacity of the active species on a support is significant for us to consider the amount of the activity component. It is suggested that the surface coverage of a catalyst by the active component can be an index of catalytic activity [25]. The optimal content of the active component is often near its dispersion capacity [26–28]. For example, B.M. Reddy et al. approached the catalytic properties of MoO_3/TiO_2 by methanol oxidation, and results show that the highest conversion to formaldehyde is at 8 wt.% loading, which is close to the theoretical dispersion capacity of MoO_3 on titania (47 m^2/g), i.e. 7.52 wt.% [28]. Many examples in catalytic applications suggest that the dispersion capacity be correlated with the catalytic properties intimately. So, measuring and discussing the dispersion capacities of supported catalysts is of obvious significance.

Recently, we have found that the dispersion amount of copper oxide on CuO/TiO_2 (anatase) varied with the impregnation times. However, the dispersion capacity of copper oxide on CuO/TiO_2 (anatase) was close to a fixed value, e.g. dispersion capacity and this result implied the fact that exploring the theoretical dispersion capacity of the supported catalysts should be significant. In this work, a series of CuO/TiO_2 with one-step and double-step impregnation have been prepared, and we will focus our attention on studying the influences of impregnation times on the dispersion of copper oxide on the anatase as well as the relationship of the dispersed copper oxide on titania (anatase) and the catalytic activities of NO + CO.

2. Experimental

2.1. Catalyst preparation

Anatase support was prepared via hydrolysis of titanium alkoxides, the product was washed, dried and then calcined in flowing air at 500 °C for 5 h [29]. The Brunauer–Emmett–Teller (BET) surface area is 77 m^2 g^{-1}.

CuO/TiO_2 samples with one-step impregnation were prepared by impregnating TiO_2 support with an aqueous solution containing the requisite amount of $Cu(NO_3)_2$, then dried at 100 °C followed by calcinations at 450 °C in air for 4 h. CuO/TiO_2 samples with double-step impregnation were prepared by impregnating CuO/TiO_2 with the copper oxide loading amount of 0.4 mmol/100 m^2 TiO_2 with the requisite amount of $Cu(NO_3)_2$, then dried at 100 °C followed by calcinations at 450 °C in air for 4 h. For the sake of simplicity, CuO/TiO_2 samples with one-step impregnation were signed as I-Cu-*x*, i.e. I-Cu-1.4 is corresponding to CuO/TiO_2 sample with one-step impregnation and CuO loading amount of 1.4 mmol/100 m^2 TiO_2. CuO/TiO_2 samples with twice impregnation were signed as II-Cu-*x*.

2.2. Instrument

X-ray diffraction (XRD) qualitative and quantitative analysis were carried out on a Philips X'pert Pro diffractometer using Ni-filtered Cu Kα radiation (0.15418 nm). The X-ray tube was operated at 40 kV and 40 mA.

Brunauer–Emmett–Teller surface areas were measured by nitrogen adsorption at 77 K on a Micromeritics ASAP 2000.

X-ray photoelectron spectroscopy (XPS) results were obtained by using a V.G. Escalab MK II spectrometer equipped with a hemispherical electron analyzer. The system was operated at 13 kV and 20 mA using a magnesium anode (Mg Kα, E = 1253.6 eV). A binding energy (BE) of 284.5 eV for the C1s level was used as an internal reference.

Temperature-programmed reduction (TPR) was carried out in a quartz U-tube reactor, and 100 mg sample was used for each measurement. Prior to the reduction, the sample was pretreated in an N_2 stream at 100 °C for 1 h, and then cooled to room temperature. After that, H_2–Ar mixture (7% H_2 by volume) was switched on and the temperature was increased linearly at a rate of 10 °C min^{-1}. A thermal conductivity cell detected the consumption of H_2 in the reactant stream.

The activities of the catalysts for NO + CO reaction were carried out under steady state, involving a feed stream with a fixed composition, NO 3.33%, CO 6.67% and He 90% by volume as diluter. A quartz tube was employed as the reactor and the requisite quantity of catalysts (20 mg for each test) was used. The catalysts were pretreated in N_2 stream at 100 °C for 1 h, and then heated to reaction temperature, after that, the mixed gases were switched on. The reactions were carried out at 300 °C with the same space velocity of 30000 ml g^{-1} h^{-1}. Two volumes and thermal conduction detector (TCD) were used for the purpose of analyzing the production, volume A with Porapak Q for separating N_2O and CO_2, and volume B with 13× molecular sieve (30–60 M) for separating N_2, NO and CO.

3. Results and discussion

Fig. 1 shows the XRD results of a series of I-Cu-*x* samples of different copper oxide loading amounts with one-step impregnation. For CuO/TiO_2 samples with low copper oxide loading amount, such as I-Cu-0.2 sample, there are no typical diffraction peaks of crystalline CuO in the pattern of Fig. 1a, except those of TiO_2 support. The typical peaks of crystalline CuO appear when the copper oxide loading amounts are beyond 0.6 mmol CuO/100 m^2 TiO_2, which indicates that crystalline CuO formed in these samples. The straight line determined by XRD quantitative analysis representing the relationship of I_{CuO}/I_{TiO_2} versus the copper oxide loading amount gives an intercept corresponding to the dispersion capacity of copper oxide on TiO_2 [30,31], and the results show that the dispersion capacity of copper oxide on TiO_2 with one-step impregnation is about 0.52 mmol CuO/100 m^2 TiO_2, as shown in Fig. 2, which approximate to the quantitative results in reference [24].

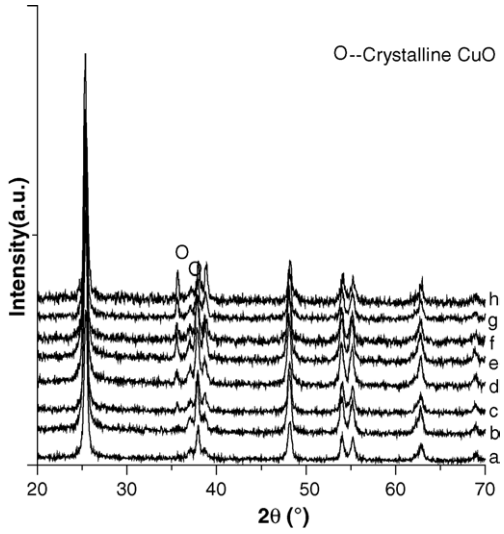

Fig. 1. (a–h) XRD patterns for I-Cu-*x* samples with copper oxide loading amounts of 0.2, 0.6, 1.0, 1.4, 1.8, 2.2, 2.5 and 3.0 mmol/100 m^2 TiO_2, respectively.

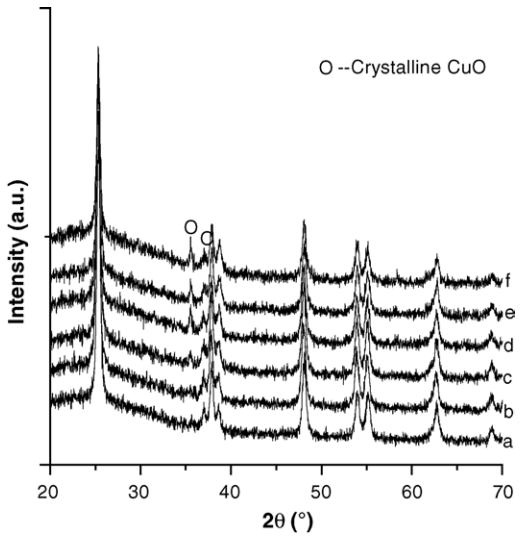

Fig. 3. (a–f) XRD patterns for II-Cu-*x* samples with copper oxide loading amounts of 0.4, 0.8, 1.4, 1.8, 2.2 and 2.6 mmol/100 m^2 TiO_2, respectively.

Fig. 3 shows the XRD results of a series of CuO/TiO_2 samples of different copper oxide loading amounts with double-step impregnation. When the copper oxide loading amount is below 0.8 mmol CuO/100 m^2 TiO_2, no typical characteristic peaks corresponding to crystalline CuO could be found in Fig. 3a and b. However, when the copper oxide loading amounts are beyond 1.4 mmol CuO/100 m^2 TiO_2, the characteristic peaks of crystalline CuO appeared in the patterns of Fig. 3e–f and their intensity increased with the copper oxide loadings. XRD quantitative results indicate that the dispersion capacity of copper oxide on anatase with double-step impregnation is about 0.98 mmol/100 m^2 TiO_2, as shown in Fig. 4. These results indicate that, for CuO/TiO_2 samples, the dispersion capacity of copper oxide on anatase with double-step impregnation is higher than that with one-step impregnation.

Figs. 5 and 6 show the TPR results of I-Cu and II-Cu samples, respectively. For these samples, when temperature is below 400 °C, two reduction peaks at about 165 and 230 °C can be detected, which could be attributed to the reduction of dispersed copper oxide and crystalline copper oxide, respectively [30]. For I-Cu and II-Cu samples, the peak area attributed to the reduction of dispersed copper oxide would reach the maximum with the copper oxide loading amount, while the area of the peak attributed to the reduction of crystalline CuO would increase with the copper oxide loading amount. When the copper oxide loading amount is beyond 2.2 mmol/100 m^2 TiO_2, it could be seen in Figs. 5f–g and 6e–f that the low temperature peak area almost keep stable. Quantitative analysis of the TPR results of these four samples, i.e. I-Cu-2.2, I-Cu-3.0, II-Cu-2.2 and II-Cu-2.6, has been carried out. Table 1 presents the proportion of two reduction peak areas in these four samples. As presented in Table 1, the dispersion capacities of copper

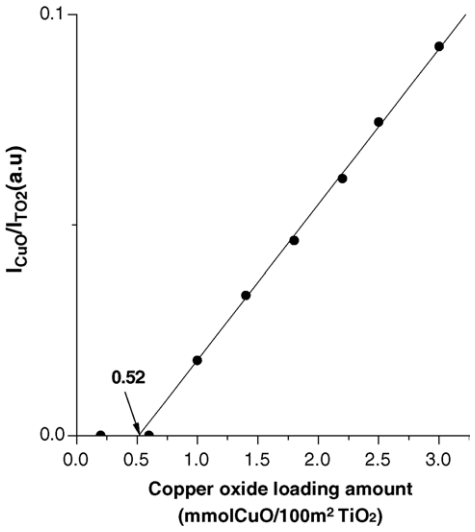

Fig. 2. Quantitative XRD results of I-Cu-*x* samples.

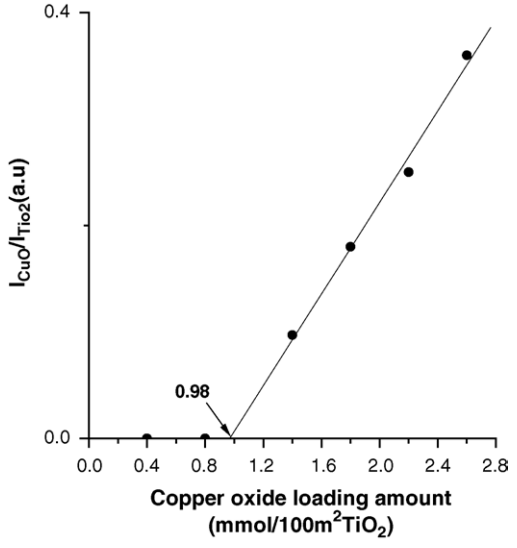

Fig. 4. Quantitative XRD results of II-Cu-*x* samples.

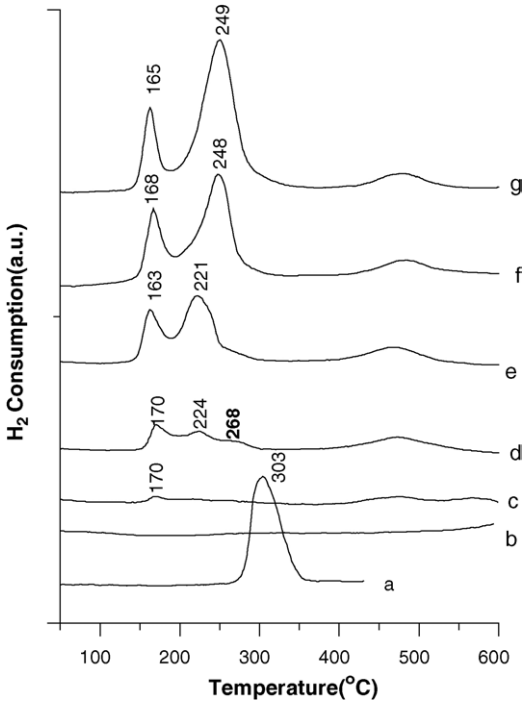

Fig. 5. TPR profiles of I-Cu-*x* samples: (a) pure CuO; (b) anatase; (c–g) copper oxide loading amounts of 0.2, 0.6, 1.4, 2.2 and 3.0 mmol/100 m^2 TiO_2, respectively.

oxide on anatase in I-Cu and II-Cu samples are about 0.54 and 0.92 mmol/100 m^2 TiO_2, which is basically consistent with XRD quantitative results, i.e. 0.52 and 0.98 mmol/100 m^2 TiO_2. In addition, it can be clearly seen that, for I-Cu samples, the reduction temperature of crystalline CuO shift from 224 to 249 °C with the copper oxide loading amount increasing from 0.6 to 3.0 mmol/100 m^2 TiO_2, and the reduction temperature of crystalline CuO in II-Cu samples increase slightly with the copper oxide loading amount. This can be understood by taking into consideration that TiO_2 is an n-type semiconductor. Under a reducing atmosphere, TiO_2 tends to produce a high concentration of n-type defects, i.e. Ti^{3+} ions and oxygen vacancies on the surface, and by donating electric charges to the Cu^{2+} ions, the unstable surface Ti^{3+} ions are returned to Ti^{4+} and the reduction of copper oxide species is promoted [32–34]. So, the enhancement of the reducibility of copper oxide species should be related to the interaction between the copper oxide species with TiO_2 support. Apparently, compared with the unsupported crystalline CuO species, dispersed copper oxide species are in close contact with the surface of TiO_2, thus the strongest influence of TiO_2 and the lowest reduction temperature are expected. For crystalline CuO, the interaction between small CuO particle and anatase should be stronger than that between large CuO particle and anatase. Thus, the reducibility of small CuO particle is enhanced more.

Table 1
Area percent of each reduction peak in TPR results

Sample	CuO loading (mmol/100 m^2 TiO_2)	Area (%)	
		Low temperature peak	High temperature peak
I-Cu	2.2	26.0	74.0
	3.0	17.3	82.7
II-Cu	2.2	40.5	59.5
	2.6	36.3	63.7

Fig. 7 shows $Cu2p_{3/2}$ XPS results of II-Cu-*x* samples. The $Cu2p_{3/2}$ binding energy of copper oxide species in II-Cu samples shift from 932.1 to 933.8 eV with the copper oxide loading amount increasing from 0.4 to 2.6 mmol/100 m^2 TiO_2. Table 2 presents the $Cu2p_{3/2}$ binding energy of some copper-contain compounds. It has been well established that for copper species

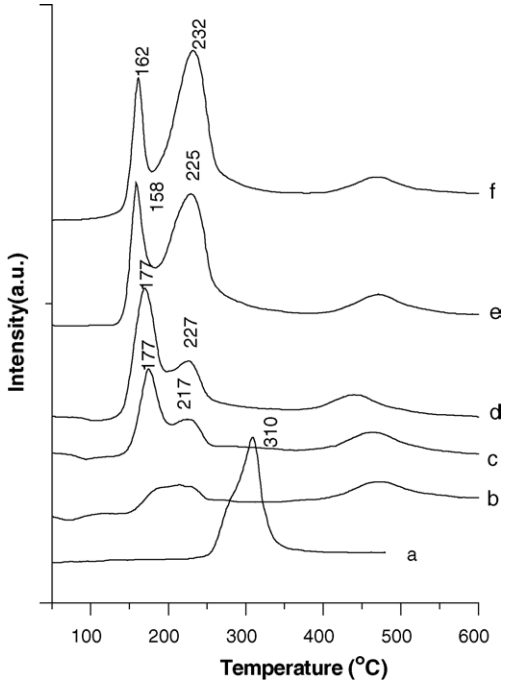

Fig. 6. TPR profiles of II-Cu-*x* samples: (a) pure CuO; (b–f) copper oxide loading amounts of 0.4, 0.8, 1.4, 2.2 and 2.6 mmol/100 m^2 TiO_2, respectively.

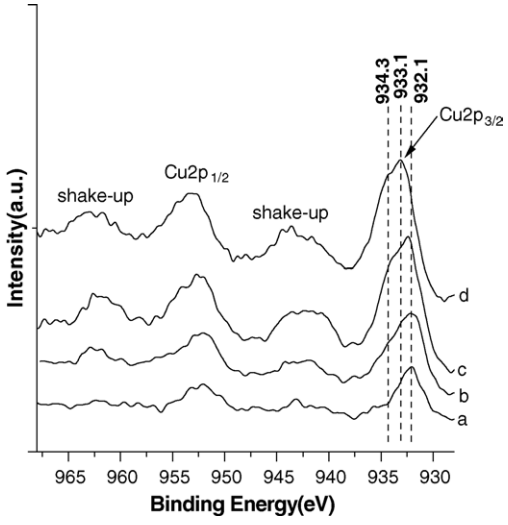

Fig. 7. Cu2p XPS spectra of II-Cu-*x* samples: (a–d) the copper oxide loading amount of 0.4, 0.8, 1.4 and 2.2 mmol/100 m^2 TiO_2, respectively.

Table 2
Binding energy of some compounds

Compound	$Cu2p_{2/3}$ (eV)
CuO	934.4
Cu_2O	932.6

Cited from [41].

the presence and absence of the shake-up peak are the characteristic for Cu^{2+} species and Cu^{+} species [35]. As shown in Fig. 7, the intensity of the $Cu2p_{3/2}$ shake-up peak of II-Cu samples increases with the copper oxide loading amount. And the $Cu2p_{3/2}$ binding energies of copper species in II-Cu-0.4 and II-Cu-0.8 are about 932.1 eV, which is similar to the Cu^{+} in Cu_2O. This result seems to suggest that copper species in these two samples mainly exist as Cu^{+} species. However, the $Cu2p_{3/2}$ binding energies of copper species in II-Cu-1.4 and II-Cu-2.2 are about 933.1 and 934.3 eV, close to the Cu^{2+} and the shake-up peak can be observed evidently, which should be attributed to the dispersed copper species and crystalline CuO. The result suggests that copper species mainly exist as the Cu^{2+} species and the crystalline CuO can be detected in II-Cu-1.4 and II-Cu-2.2. These results also indicate that the dispersion capacity of copper oxide on anatase with double impregnations is higher than 0.8 mmol/100 m^2 TiO_2 and lower than 1.4 mmol/100 m^2 TiO_2. As reported by Andersson and Larsson [19], dispersed Cu^{2+} species on anatase would be reduced to Cu^{+} species during the XPS measurement and the amount of Cu^{+} species would increase with the analysis time. Therefore, the creation of Cu^{+} species should be related to the reduction of dispersed Cu^{2+} species. In addition, for II-Cu-1.4 and II-Cu-2.2 samples, the $Cu2p_{3/2}$ binding energy of dispersed Cu^{2+} species is about 933.1 eV, which is lower than that of Cu^{2+} ions in crystalline CuO, 934.3 eV. The shift might be related to the intensity of Cu–O bond, i.e. the intensity of Cu–O bond of dispersed Cu^{2+} species in CuO/TiO_2 sample might be weaker than that of Cu^{2+} in crystalline CuO.

Shown in Fig. 8 are the NO + CO activity and N_2 selectivity of a series of I-Cu and II-Cu samples. For I-Cu-*x* samples, the NO + CO activities decrease slowly with the presence of crystalline CuO. When the copper oxide loading amounts are lower than its dispersion capacity on anatase with double impregnations, such as II-Cu-0.4 and II-Cu-0.8 samples, the NO + CO activity and N_2 selectivity increase with the copper oxide loading; when the copper oxide loading amounts are beyond its dispersion capacity on anatase, such as II-Cu-1.4 and II-Cu-2.2 samples, the NO + CO activity keeps stable and the N_2 selectivity decreases slightly with the copper oxide loading amounts. The activity increases with the amount of dispersed copper oxide, indicating that dispersed copper oxide species might be the active species in these catalysts at current conditions. Therefore, it could be concluded that increasing the dispersed copper oxide amount could enhance the activities of these catalysts.

Xie et al. have investigated the influence of different precursors on the dispersion capacity of NiO and MoO_3 on γ-Al_2O_3. The results suggest that as a relatively low melting point oxide, MoO_3 gives out a higher dispersion capacity than its precursor molybdate used for impregnations; as a high melting point oxide, the dispersion capacity of NiO is the same as that of its precursors [36]. Along this line, the dispersion capacity of CuO on anantase should be related to the dispersion capacity of $Cu(NO_3)_2$. As discussed previously [29,37], the (0 0 1) plane of the TiO_2 (anatase) is considered the preferentially exposed plane, the dispersion capacity and the surface states of the active species could be expected by considering the surface structure of TiO_2. For anatase, the vacant site density in (0 0 1) plane is about 1.16 mmol/100 m^2, shown in Fig. 9a. When anatase was impregnated by $Cu(NO_3)_2$ aqueous solution, Cu^{2+} ions would occupy the vacant site on anatase surface and the two accompanying NO_3^- anion would stay at the top of the occupied site as capping NO_3^-, compensating the extra positive charge. As reported elsewhere [38], the effect radius and area of NO_3^- is about 0.19 nm and 0.125 nm^2, respectively. The two accompanying NO_3^- anion would prevent some of the neighboring vacant sites on the surface of anatase from being incorporated by other copper ions, as shown in Fig. 9b. Considering this shielding effect of capping NO_3^- anion, when the NO_3^- anions form a close-pack monolayer on the anatase surface, the dispersion capacity of $Cu(NO_3)_2$ on anatase is about 0.66 mmol/100 m^2 TiO_2. During the calcinations, dispersed $Cu(NO_3)_2$ would decompose and form dispersed CuO species and those vacant sites shielded by capping NO_3^- anion would expose on the surface of anatase, and the excess of $Cu(NO_3)_2$ in these samples would decompose and might mainly form crystalline CuO. Accordingly, for the CuO/TiO_2 samples with one-step impregnation, the dispersion capacity of

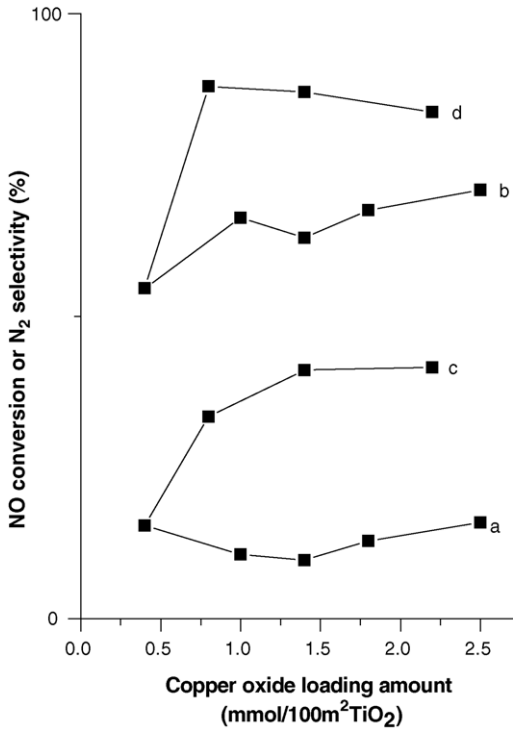

Fig. 8. Relationship between the NO conversions or the N_2 selectivity and the copper oxide loading amount: (a and c) the NO conversion of I-Cu-*x* and II-Cu-*x*; (b and d) the N_2 selectivity of I-Cu-*x* and II-Cu-*x* samples, respectively.

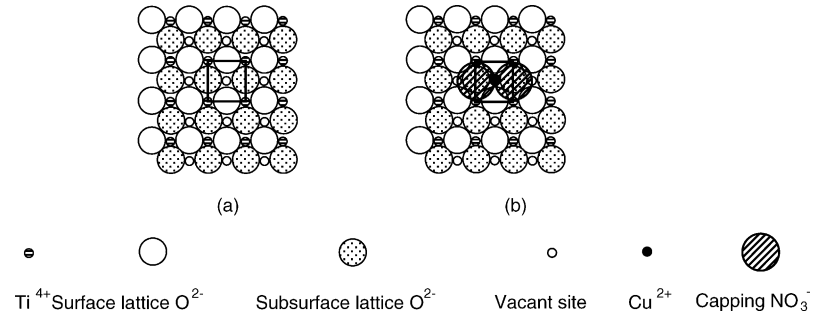

Fig. 9. The schematic diagram for the incorporated Cu^{2+} ions in the surface vacant sites on the (0 0 1) plane of TiO_2 (anatase): (a) (0 0 1) plane of TiO_2 (anatase) and (b) incorporation of the dispersed Cu^{2+} species accompanying with two NO_3^- anions on the (0 0 1) plane of TiO_2 (anatase) support.

copper oxide on anatase is basically equal to the dispersion capacity of $Cu(NO_3)_2$ on anatase, i.e. about 0.66 mmol/100 m^2 TiO_2. This is different from other systems, such as CuO/CeO_2, $CuO/\gamma\text{-}Al_2O_3$, etc. In CuO/CeO_2, $CuO/\gamma\text{-}Al_2O_3$ systems, the excess of $Cu(NO_3)_2$ might decompose and form dispersed copper oxide species on the surface of support, thus copper oxide monolayer dispersion on these support could be reached after one-step impregnation [39,40]. The different behavior of the excess of $Cu(NO_3)_2$ between in CuO/TiO_2 system and other systems might be related to the difference of the interaction extent between the dispersed copper oxide species and the support. For I-Cu-0.4 support after calcinations, the vacant site unoccupied by Cu^{2+} ions is around 0.76 mmol/100 m^2 TiO_2, which can be expected by the incorporation model. When I-Cu-0.4 was impregnated one more time by $Cu(NO_3)_2$ aqueous solution, $Cu(NO_3)_2$ would occupy those remained vacant sites on the surface of I-Cu-0.4. Similarly, considering the shielding effect of capping NO_3^- anion, the dispersion capacity of $Cu(NO_3)_2$ on I-Cu-0.4 is about 0.66 mmol/100 m^2 TiO_2. After calcinations, the dispersion capacity of copper oxide on anatase is about 1.06 mmol/100 m^2 TiO_2, which is basically coincided with the XRD and quantitative TPR results.

4. Conclusion

Double-step impregnation could enhance the dispersion capacity of copper oxide on the surface of anatase and the maximal monolayer dispersion capacity of copper oxide on the surface of anatase is 1.16 mmol/100 m^2 TiO_2, which is expected by incorporation model. The activities of CuO/TiO_2 catalysts for NO + CO reaction at 300 °C are close related to disperse copper oxide species. It could be predicted that the CuO/TiO_2 catalysts with double and multiple impregnations would show the better activity than those with one-step impregnations.

Acknowledgements

The financial supports of the Special of Foundation for the Doctor-subject of China (No. 20030284002) and the National Basic Research Program of China (Grant No. 2003CB615804) are gratefully acknowledged.

References

[1] H.P. Boehm, H. Knozinger, in: J.R. Anderson, M. Boudart (Eds.), Analysis, Science and Technology, vol. 4, Springer–Verlag, West Berlin, 1983, p. 39.
[2] Y.I. Yermakov, B.N. Kuznetsov, V.A. Zakharov, Analysis by Supported Complexes, Elsevier, Amsterdam, 1981.
[3] B. Delmon, M. Houalla, in: B. Delmon, P. Grange, P.A. Jacobs, G. Poncesteplet (Eds.), Preparaton of Catalysts II, Elsevier, Amsterdam, 1979, p. 447.
[4] H. Knozinger, E. Taglauer, in: J.J. Spivey, S.K. Agarwal (Eds.), Catalysis, A Specialist Periodical Report, vol. 10, The Royal Society of Chemistry, London, 1993, p. 1.
[5] F.E. Massoth, Adv. Catal. 27 (1978) 265.
[6] L. Dong, Y. Hu, F. Xu, D. Lu, B. Xu, Z. Hu, Y. Chen, J. Phys. Chem. 104 (2000) 78.
[7] L. Dong, Y. Hu, M. Shen, T. Jin, J. Wang, W. Ding, Y. Chen, Chem. Mater. 13 (2001) 4227.
[8] B.L. Xu, Y.N. Fan, L. Liu, M. Lin, Y. Chen, Sci. China Ser. B 45 (2002) 407.
[9] D.J. Cole, C.F. Cullis, D.J. Hucknall, J. Chem. Soc. Faraday Trans. I 72 (1976) 2185.
[10] K.Y.S. Ng, E. Gulari, J. Catal. 92 (1985) 340.
[11] Y.C. Liu, G.L. Griffin, S.S. Chan, J. Catal. 94 (1985) 108.
[12] R.T. Rewick, H. Wise, J. Catal. 40 (1975) 301.
[13] F. Boccuzzi, E. Guglielminotti, G. Martra, G. Cerrato, J. Catal. 146 (1994) 449.
[14] M.C. Wu, D.W. Goodman, J. Phys. Chem. 98 (1994) 9874.
[15] H. Knozinger, Adv. Catal. 25 (1976) 184.
[16] G.C. Chinchen, K.C. Waugh, J. Catal. 97 (1986) 280.
[17] T.H. Fleisch, R.L. Mieville, J. Catal. 97 (1986) 284.
[18] P. Larsson, A. Andersson, L.R. Wallenberg, B. Svensson, J. Catal. 163 (1996) 279.
[19] P. Larsson, A. Andersson, J. Catal. 179 (1998) 72.
[20] P.Y. Lin, M. Skoglundh, L. Lowendahl, J.E. Otterstedt, L. Dahl, K. Jansson, M. Nygren, Appl. Catal. B 6 (1995) 237.
[21] J.W. London, A.T. Bell, J. Catal. 31 (1973) 96.
[22] R. Hierl, H.P. Urbach, H. Knozinger, J. Chem. Soc. Faraday Trans. 88 (1992) 355.
[23] A.R. Balkenede, H. den Daas, M. Huisman, O.L.J. Gijzeman, J.W. Geus, Appl. Surf. Sci. 47 (1991) 341.
[24] X. Yu, N. Wu, Y. Xie, Y. Tang, J. Mater. Chem. 10 (2000) 1629.
[25] S. Rondon, M. Houalla, D.M. Hercules, Surf. Interface Anal. 26 (1998) 329.
[26] K.V. Narayana, A. Venugopal, K.S. Rama Rao, S. Khaja Masthan, V. Venkat Rao, P. Kanta Rao, Appl. Catal. A 167 (1998) 11.
[27] K.V. Narayana, A. Venugopal, K.S. Rama Rao, V. Venkat Rao, S. Khaja Masthan, P. Kanta Rao, Appl. Catal. A 150 (1997) 269.
[28] B.M. Reddy, K. Narsimha, P. Kanta Rao, Langmuir 7 (1991) 1551.
[29] H. Zhu, M. Shen, Y. Kong, J. Hong, Y. Hu, T. Liu, L. Dong, Y. Chen, C. Jian, Z. Liu, J. Mol. Catal. A 219 (2004) 155.

[30] B. Xu, L. Dong, Y. Chen, J. Chem. Soc. Faraday Trans. 94 (1998) 1905.
[31] Y.C. Xie, Y.Q. Tang, Adv. Catal. 37 (1990) 1.
[32] S.J. Decanlo, T.M. Apple, C.R. Dybowski, J. Phys. Chem. 87 (1983) 194.
[33] P. Meriaudeau, O.M. Ellested, C. Naccache, J. Catal. 75 (1982) 243.
[34] D. Duprez, A. Miloudi, Stud. Surf. Sci. Catal. 11 (1982) 179.
[35] D. Brigs, M.P. Seah (Eds.), Practical Surface Analysis by Auger and X-ray Photoelectron Spectroscopy, Wiley, New York, 1983.
[36] X. Wang, B. Zhao, D. Jiang, Y. Xie, Appl. Catal. A 188 (1999) 201.
[37] B. Xu, L. Dong, Y.N. Fan, Y. Chen, J. Catal. 193 (2000) 88.
[38] J.T. Cheng, P.D. Ellis, J. Phys. Chem. 93 (1989) 2549.
[39] L. Dong, Y. Jin, Y. Chen, Sci. China Ser. B 40 (1997) 24.
[40] L. Dong, Y. Hu, M. Shen, T. Jin, J. Wang, W. Ding, Y. Chen, Chem. Mater. 13 (2001) 4227.
[41] X. Jiang, L. Lou, Y. Chen, X. Zheng, J. Mol. Catal. A Chem. 197 (2003) 193.